J|A|C|S
ARTICLES
Published on Web 07/29/2006

Synthesis and Characterization of the Octahydrotriborate Complexes $Cp^*V(B_3H_8)_2$ and $Cp^*Cr(B_3H_8)_2$ and the Unusual Cobaltaborane Cluster $Cp^*_2Co_2(B_6H_{14})$

Do Young Kim and Gregory S. Girolami*

Contribution from the School of Chemical Sciences, University of Illinois at Urbana−Champaign, 600 South Mathews Avenue, Urbana, Illinois 61801

Received May 10, 2006; E-mail: girolami@scs.uiuc.edu

Abstract: The new compounds $Cp^*V(B_3H_8)_2$, $Cp^*Cr(B_3H_8)_2$, and $Cp^*_2Co_2(B_6H_{14})$ have been synthesized by treating the pentamethylcyclopentadienyl complexes $[Cp^*VCl_2]_3$, $[Cp^*CrCl_2]_2$, and $[Cp^*CoCl]_2$ with NaB_3H_8. X-ray crystallography shows that $Cp^*V(B_3H_8)_2$ and $Cp^*Cr(B_3H_8)_2$ have the same ligand sets but different molecular structures: the vanadium compound contains two bidentate B_3H_8 ligands (i.e., bound to the metal center via two vicinal hydrogen atoms), whereas the chromium compound has one bidentate B_3H_8 ligand and one B_3H_8 ligand bound in an unprecedented fashion via two geminal hydrogen atoms. The "gem-bound" B_3H_8 group itself has an atypical structure consisting of a $BH_2-BH_2-BH_3$ triangle with one additional hydrogen atom bridging the unique BH_2-BH_2 edge. The B−B distances are nearly identical within experimental error at 1.790(5), 1.792(5), and 1.786(6) Å. The relationship between the electronic and molecular structures of the V and Cr compounds is briefly discussed. The structure of $Cp^*_2Co_2(B_6H_{14})$ can be viewed in two different ways: as a dicobalt complex in which two Cp*Co units are each bound to four adjacent boron atoms of an S-shaped B_6H_{14} ligand, or as an eight-vertex *hypho* cluster compound. In the former case, the B_6H_{14} ligand is best regarded as a dianionic bi-borallyl group $H_3B(\mu-H)BH(\mu-H)BHBH(\mu-H)BH(\mu-H)BH_3$ in which one hydrogen at each end of the chain is involved in an agostic interaction. From a cluster point of view, the structure of $Cp^*_2Co_2(B_6H_{14})$ can be generated by removing three adjacent high-connectivity vertices from the eleven-vertex *closo* polyhedron. The Co−B distances vary from 2.008(5) to 2.183(4) Å, and the B−B distances within in the S-shaped chain range from 1.734(8) to 1.889(6) Å. Finally, a new synthesis of the known molybdenum compound $Cp^*_2Mo_2(B_5H_9)$ is described; its structure as established by X-ray crystallography closely resembles that of the previously described (C_5H_4Me) analogue.

Introduction

Transition metal diborides such as TiB_2, ZrB_2, and HfB_2 have outstanding properties for microelectronic, coating, and other applications: their melting points exceed 3000 °C, their bulk resistivities are near 15 $\mu\Omega\cdot$cm,[1] their bulk hardness approaches 30 GPa,[1] and they have excellent corrosion resistance.[2] These metallic ceramics perform well as copper diffusion barriers for microelectronics[3−7] but are not currently used for this purpose, in part because suitable low-temperature, halide-free deposition processes were unavailable until very recently. We and others, however, have demonstrated that transition metal tetrahydroborate complexes, $M(BH_4)_x$, are highly effective single-source precursors for the chemical vapor deposition (CVD) of metal diboride thin films.[3,4,8] These BH_4 precursors are attractive because they contain the requisite elemental components and are free of heteroatoms that could contaminate the films.

Unfortunately, among the d-block transition metals, only Ti,[9] Zr,[10] and Hf[10] form volatile $M(BH_4)_x$ complexes in which all the ligands are BH_4 groups. Volatile MB_xH_y complexes of other elements should be obtainable by using sterically more demanding boron hydride ligands, and to this end, we have recently begun to investigate the chemistry of the largely unexplored octahydrotriborate anion, $B_3H_8^-$. We have reported the synthesis and characterization of the remarkable chromium(II) complex $Cr(B_3H_8)_2$[11] and have shown that this compound is highly volatile and is an excellent (in fact, the first) single-source precursor to very high quality CrB_2 thin films at remarkably low temperatures (200 °C).[12]

(1) Kieffer, R.; Benesovsky, F. *Hartstoffe*; Springer: Vienna, 1963.
(2) Castaing, J.; Costa, P. In *Boron and Refractory Borides*; Matkovich, V. I., Ed.; Springer: New York, 1977; pp 390−412.
(3) Sung, J.; Goedde, D. M.; Girolami, G. S.; Abelson, J. R. *J. Appl. Phys.* **2002**, *91*, 3904−3911.
(4) Jayaraman, S.; Yang, Y.; Kim, D. Y.; Girolami, G. S.; Abelson, J. R. *J. Vac. Sci. Technol., A* **2005**, *23*, 1619−1625.
(5) Williams, L. M. *J. Electrochem. Soc.* **1986**, *133*, C225−C225.
(6) Chen, J. S.; Wang, J. L. *J. Electrochem. Soc.* **2000**, *147*, 1940−1944.
(7) Lin, S. T.; Kuo, Y. L.; Lee, C. *Appl. Surf. Sci.* **2003**, *220*, 349−358.
(8) Jensen, J. A.; Gozum, J. E.; Pollina, D. M.; Girolami, G. S. *J. Am. Chem. Soc.* **1988**, *110*, 1643−1644.
(9) Hoekstra, H. R.; Katz, J. J. *J. Am. Chem. Soc.* **1949**, *71*, 2488−2492.
(10) Reid, W. E. J.; Bish, J. M.; Brenner, A. *J. Electrochem. Soc.* **1957**, *104*, 21−29.
(11) Goedde, D. M.; Girolami, G. S. *J. Am. Chem. Soc.* **2004**, *126*, 12230−12231.

Table 1. Crystallographic Data for $Cp^*V(B_3H_8)_2$ (**1**), $Cp^*Cr(B_3H_8)_2$ (**2**), and $Cp^*_2Co_2(B_6H_{14})$ (**3**)

	1	2	3	4
formula	$VB_6C_{10}H_{31}$	$CrB_6C_{10}H_{31}$	$Co_2B_6C_{20}H_{44}$	$Mo_2B_5C_{20}H_{39}$
formula weight	267.15	268.22	467.27	525.44
T, °C	−80	−80	−80	−80
space group	$C2/m$	$Pbcn$	$P4_12_12$	$P\bar{1}$
a, Å	7.745(3)	15.517(3)	8.7060(10)	8.998(2)
b, Å	16.065(6)	15.489(3)	8.7060(10)	11.701(3)
c, Å	7.513(3)	14.462(3)	32.496(7)	11.971(3)
α, deg	90	90	90	109.562(4)
β, deg	116.825(5)	90	90	91.892(4)
γ, deg	90	90	90	92.495(4)
V, Å^3	834.1(6)	3475.7(13)	2463.0(7)	1185.0(5)
Z	2	8	4	2
ρ_{calcd}, g cm^{-3}	1.064	1.025	1.260	1.473
λ, Å	0.71073	0.71073	0.71073	0.71073
μ_{calcd}, cm^{-1}	5.69	6.34	13.51	1.061
transmission coeff	N/A	0.936−0.799	0.974−0.753	0.896−0.833
R_F[a]	0.0700	0.0351	0.0358	0.0357
R_{wF2}[b]	0.0993	0.0693	0.0661	0.0652

[a] $R_F = \sum||F_o| - |F_c||/\sum|F_o|$ for reflections with $F_o^2 > 2\,\sigma(F_o^2)$. [b] $R_{wF2} = [\sum w(F_o^2 - F_c^2)^2/\sum w(F_o^2)^2]^{1/2}$ for all reflections.

We now describe our efforts to synthesize and characterize new B_3H_8 complexes that also bear cyclopentadienyl ligands. Specifically, we report the reactions of the pentamethylcyclopentadienyl complexes $[Cp^*VCl_2]_3$, $[Cp^*CrCl_2]_2$, $[Cp^*CoCl]_2$, and $[Cp^*MoCl_2]_2$ with NaB_3H_8 and the characterization of the respective products. One of the new molecules, $Cp^*Cr(B_3H_8)_2$, exhibits an unprecedented bonding mode for the B_3H_8 ligand in which the anion is bound to the metal via two geminal hydrogen atoms. We also describe the formation of the dinuclear complex $Cp^*_2Co_2(B_6H_{14})$, which can be considered either as a "bi-borallyl" complex or as an eight-vertex *hypho* cluster.

Results

Synthesis and Characterization of $Cp^*V(B_3H_8)_2$. Treatment of the vanadium(III) "half-sandwich" starting material $[Cp^*VCl_2]_3$ with excess NaB_3H_8 in diethyl ether, followed by pentane extraction and crystallization at −20 °C, affords light green crystals of the new vanadium(III) complex $Cp^*V(B_3H_8)_2$ (**1**)

$$^1/_3\,[Cp^*VCl_2]_3 + 2\,NaB_3H_8 \rightarrow Cp^*V(B_3H_8)_2 + 2\,NaCl \quad (1)$$

The IR spectrum of **1** features strong bands at 2517 and 2467 cm^{-1} due to terminal B−H stretches, and strong bands at 2131, 2082, and 2044 cm^{-1} due to bridging B−H stretches. The pattern of bands is similar to that seen for bidentate B_3H_8 ligands in other complexes.[11,13] The magnetic moment of 2.7 μ_B in benzene measured by Evans' method indicates the presence of two unpaired electrons per vanadium center, as expected for the V^{III} oxidation state.

The molecular structure of **1** is shown in Figure 1; crystal data and important bond distances and angles are listed in Tables 1 and 2. We point out here that the crystal exhibits an unusual form of disorder, but despite this aspect the molecular structure is clearly defined (see Experimental Section for details). The vanadium center is coordinated to two bidentate B_3H_8 groups and to one η^5-Cp* ligand; the overall geometry is that of a four-legged piano stool. The B_3H_8 ligands adopt their usual structure: an isosceles triangle in which two of the edges are bridged by a hydrogen atom. The B−B distances are 1.755(11) Å for the nonbridged B−B bond and 1.837(18) and 1.870(16) Å for the two bridged B−B bonds. Each of the three boron atoms bears two terminal hydrogen atoms, one above the B_3 plane and one below. Both B_3H_8 groups coordinate to the V center in the same way: by means of one terminal hydrogen atom on each of the two boron atoms at the ends of the nonbridged B−B bond. The average V−H distance is 2.14(6) Å, and the average V···B distance is 2.580(8) Å. The B_3 plane of the B_3H_8 ligand and the VB_2 plane formed with the two boron atoms bound to vanadium form a dihedral angle of 119.7(5)°, which is similar to the dihedral angles observed in other metal B_3H_8 complexes.[14] For purposes of later discussion, we point out here that, for each B_3H_8 ligand, the Cp* and B_3 units are *cis* to one another relative to the VB_2 plane.

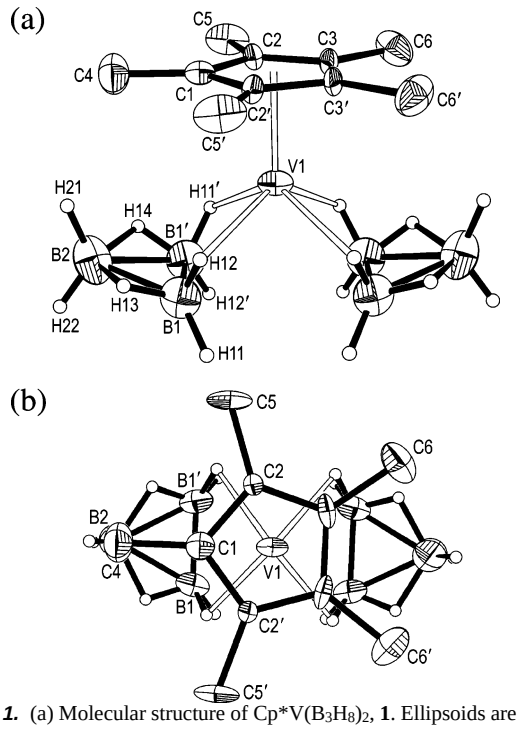

Figure 1. (a) Molecular structure of $Cp^*V(B_3H_8)_2$, **1**. Ellipsoids are drawn at the 35% probability level, except for hydrogen atoms, which are represented as arbitrarily sized spheres. Methyl hydrogen atoms in the Cp* group have been deleted for clarity. (b) Top view of **1**.

(12) Jayaraman, S.; Klein, E. J.; Yang, Y.; Kim, D. Y.; Girolami, G. S.; Abelson, J. R. *J. Vac. Sci. Technol., A* **2005**, *23*, 631−633.
(13) Gaines, D. F.; Hildebrandt, S. J. *Inorg. Chem.* **1978**, *17*, 794−806.
(14) Goedde, D. M. Transition Metal Hydroborate Complexes: Structures, Syntheses, and Use as Chemical Vapor Deposition Precursors. Ph.D. Thesis, University of Illinois at Urbana−Champaign, 2001, 181 pp.

Table 2. Important Bond Lengths (Å) and Angles (deg) for $Cp^*V(B_3H_8)_2$ (**1**)[a]

Bond Lengths (Å)			
V(1)−B(1)	2.572(7)	B(1)−H(12)	1.14(5)
V(1)−B(1)′	2.587(7)	B(1)−H(13)	1.09(2)
V(1)−H(11)′	2.19(4)	B(1)′−H(14)	1.06(4)
V(1)−H(12)	2.08(5)	B(2)−H(13)	1.35(7)
B(1)−B(1)′	1.755(11)	B(2)−H(14)	1.36(6)
B(1)−B(2)	1.870(16)	B(2)−H(21)	1.10(5)
B(1)′−B(2)	1.837(18)	B(2)−H(22)	1.07(5)
B(1)−H(11)	1.11(4)		

Bond Angles (deg)			
B(1)−V(1)−B(1)′	39.8(2)	B(2)−B(1)′−H(12)′	134(3)
B(1)−V(1)−B(1)″	80.3(2)	B(1)′−B(1)−H(13)	103(4)
B(1)−V(1)−B(1)‴	93.4(2)	B(2)−B(1)−H(13)	46(3)
B(1)−B(1)′−B(2)	60.8(7)	B(1)−B(2)−H(13)	35(2)
B(1)−B(2)−B(1)′	56.5(5)	B(1)′−B(2)−H(14)	35(2)
V(1)−B(1)−B(1)′	70.6(3)	H(11)−B(1)−H(13)	79(4)
V(1)−B(1)−B(2)	105.3(7)	H(12)−B(1)−H(13)	127(5)
B(1)′−V(1)−H(11)′	25.3(14)	H(21)−B(2)−H(22)	124(8)
B(1)−V(1)−H(12)	25.9(14)	H(14)−B(2)−H(13)	121(4)
V(1)−B(1)−H(11)	115(2)	B(1)−B(2)−H(21)	120(6)
V(1)−B(1)′−H(11)′	57(2)	B(1)′−B(2)−H(21)	119(6)
V(1)−B(1)−H(12)	53(2)	B(1)−B(2)−H(22)	108(6)
V(1)−B(1)′−H(12)′	120(2)	B(1)′−B(2)−H(22)	112(6)
H(11)−B(1)−H(12)	99(3)	H(13)−B(2)−H(21)	102(7)
B(1)′−B(1)−H(11)	125(2)	H(14)−B(2)−H(21)	99(6)
B(2)−B(1)−H(11)	140(2)	H(13)−B(2)−H(22)	99(6)
B(1)′−B(1)−H(12)	119(3)	H(14)−B(2)−H(22)	104(7)
B(2)−B(1)−H(12)	110(3)	H(21)−B(2)−H(22)	123(8)
B(2)−B(1)′−H(11)′	119(2)		

[a] Symmetry transformations used to generate equivalent atoms: ′ = 1 − *x*, *y*, −*z*; ″ = *x*, −*y*, *z*; ‴ = 1 − *x*, −*y*, −*z*.

Synthesis and Characterization of $Cp^*Cr(B_3H_8)_2$. Treatment of the chromium(III) half-sandwich starting material $[Cp^*CrCl_2]_2$ with NaB_3H_8 in diethyl ether, followed by pentane extraction and crystallization at −20 °C, affords dark green needles of $Cp^*Cr(B_3H_8)_2$ (**2**).

$$^1/_2\,[Cp^*CrCl_2]_2 + 2\,NaB_3H_8 \rightarrow Cp^*Cr(B_3H_8)_2 + 2\,NaCl \quad (2)$$

The IR spectrum of **2** features strong bands at 2482, 2456, and 2418 cm^{-1} due to terminal B−H stretches, and strong bands at 2094 cm^{-1} due to bridging B−H stretches. The magnetic moment of 4.1 μ_B in solution indicates the presence of three unpaired electrons per chromium center, as expected for Cr^{III}. The molecular structure of **2** is illustrated in Figure 2, and crystal data and important bond distances and angles for **2** are given in Tables 1 and 3. Unlike the vanadium center in **1**, the chromium center in **2** is coordinated to two *different* B_3H_8 groups. One of the B_3H_8 groups is bound in the typical bidentate fashion as seen above for the vanadium complex. The Cr−H and Cr···B distances for this ligand average 1.89(2) and 2.40(1) Å, respectively, and are similar to those of 1.87 and 2.423 Å in homoleptic $Cr(B_3H_8)_2$.[11] The dihedral angle between the B_3 plane and the CrB_2 plane is 126.7(2)°. Unlike **1**, however, the Cp* and B_3 units of the bidentate B_3H_8 ligand are *trans* to one another relative to the CrB_2 plane. In other words, the boron atom not bound to the metal center is distal to the Cp* ligand in the chromium compound but proximal to the Cp* ligand in the vanadium compound. In both cases, the geometry adopted probably minimizes the steric repulsions between the ligands.

Surprisingly, the second B_3H_8 group in **2** is bound in an unprecedented fashion. This ligand coordinates to the chromium center by means of two geminal hydrogen bridges from the *same* boron center. These hydrogen atoms, H(41) and H(42), form Cr−H contacts of 1.99(2) and 2.17(2) Å. Interestingly, the unusual binding mode is reflected in significant changes in the overall geometry of the B_3H_8 group. The structure seen for the free $B_3H_8^-$ anion and for essentially all of its coordination

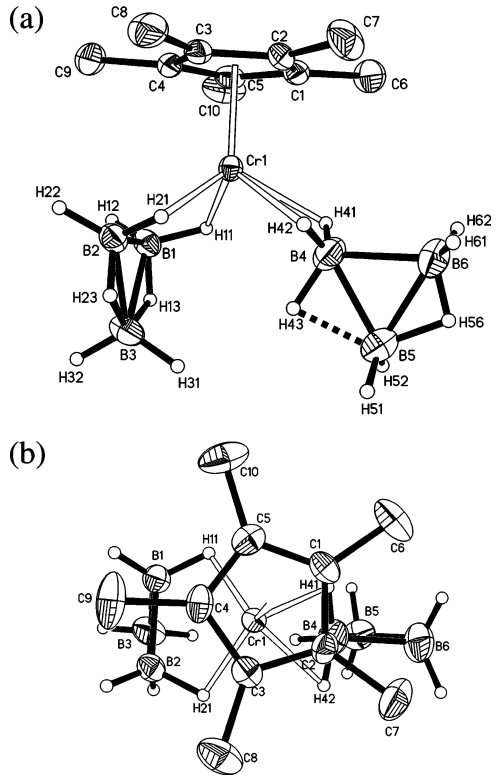

Figure 2. (a) Molecular structure of $Cp^*Cr(B_3H_8)_2$, **2**. Ellipsoids are drawn at the 35% probability level, except for hydrogen atoms, which are represented as arbitrarily sized spheres. Methyl hydrogen atoms in the Cp* group have been deleted for clarity. (b) Top view of **2**.

Table 3. Important Bond Lengths (Å) and Angles (deg) for $Cp^*Cr(B_3H_8)_2$ (**2**)

Bond Lengths (Å)			
Cr(1)−H(11)	1.90(2)	B(2)−H(22)	1.06(2)
Cr(1)−H(21)	1.870(19)	B(2)−H(23)	1.07(2)
Cr(1)−H(41)	1.99(2)	B(3)−H(13)	1.28(2)
Cr(1)−H(42)	2.17(2)	B(3)−H(23)	1.41(2)
Cr(1)−B(1)	2.392(3)	B(3)−H(31)	1.13(2)
Cr(1)−B(2)	2.409(3)	B(3)−H(32)	1.11(2)
Cr(1)−B(4)	2.347(3)	B(4)−H(41)	1.12(2)
B(1)−B(2)	1.758(4)	B(4)−H(42)	1.13(2)
B(1)−B(3)	1.828(5)	B(4)−H(43)	1.13(3)
B(2)−B(3)	1.840(4)	B(5)−H(43)	1.61(3)
B(4)−B(5)	1.790(5)	B(5)−H(51)	1.08(2)
B(4)−B(6)	1.792(5)	B(5)−H(52)	1.15(3)
B(5)−B(6)	1.786(6)	B(5)−H(56)	1.26(3)
B(1)−H(11)	1.16(2)	B(6)−H(56)	1.09(3)
B(1)−H(12)	1.04(2)	B(6)−H(61)	1.12(3)
B(1)−H(13)	1.09(3)	B(6)−H(62)	1.07(2)
B(2)−H(21)	1.188(18)		

Bond Angles (deg)			
B(4)−Cr(1)−B(1)	104.40(13)	H(31)−B(3)−H(32)	118.3(18)
B(4)−Cr(1)−B(2)	103.27(13)	B(5)−B(4)−B(6)	59.8(2)
B(1)−Cr(1)−B(2)	42.95(10)	B(6)−B(5)−B(4)	60.1(2)
H(11)−Cr(1)−H(21)	95.5(9)	B(5)−B(6)−B(4)	60.0(2)
H(41)−Cr(1)−H(42)	55.3(8)	H(41)−B(4)−H(42)	118.8(16)
B(2)−B(1)−B(3)	61.72(18)	H(41)−B(4)−H(43)	107.5(19)
B(1)−B(2)−B(3)	61.02(18)	H(42)−B(4)−H(43)	103.1(18)
B(1)−B(3)−B(2)	57.25(17)	H(51)−B(5)−H(52)	116.0(18)
H(11)−B(1)−H(12)	114.0(17)	H(61)−B(6)−H(62)	121(2)
H(21)−B(2)−H(22)	111.7(16)		

complexes (including compound **1**) is a $BH_2-BH_2-BH_2$ triangle in which additional hydrogen atoms bridge two edges. For the "gem-bound" B_3H_8 group in **2**, the structure is a $BH_2-BH_2-BH_3$ triangle with one additional hydrogen atom bridging the unique BH_2-BH_2 edge. The bridging hydrogen atom bridges relatively symmetrically: the two B−H distances are 1.26(3) and 1.09(3) Å. One of the three hydrogen atoms on the BH_3 group, H(43), may be regarded as semibridging rather than terminal: the B(4)−H(43) distance is normal at 1.13(3) Å, but the B(5)−H(43) distance of 1.61(3) Å is quite long. The B−B distances within the B_3H_8 unit are nearly identical within experimental error at 1.790(5), 1.792(5), and 1.786(6) Å; this is somewhat unusual because in other B_3H_8 ligands the two H-bridged B−B edges are typically 0.04−0.07 Å longer than the nonbridged B−B edge.[11,15] The B_3 plane of the gem-bound B_3H_8 group is almost exactly parallel to the plane that bisects the bidentate B_3H_8 group.

The arrangement of hydrogen atoms within the gem-bound B_3H_8 group most closely resembles the structures of several neutral compounds of stoichiometry $B_3H_7{\cdot}L$, where L = CO, PH_3, or NH_3.[16−18] There are, however, some significant differences. Unlike the pattern seen in **2**, in these Lewis base adducts the bridged B−B edge is considerably shorter than the other two nonbridged B−B edges, and all three of the terminal hydrogen atoms in the BH_3 unit are clearly terminal and not involved even in weak bridging interactions. The pattern of B−B distances and the locations of the hydrogen atoms suggest that the structure of the gem-bound B_3H_8 ligand in **2** is intermediate between that seen in the $B_3H_7{\cdot}L$ compounds above and that usually seen for the $B_3H_8^-$ anion, in either its free or coordinated state. Presumably, the geminal coordination mode results in an electronic structure somewhat like that in the $B_3H_7{\cdot}L$ compounds, and thereby causes changes in the preferred geometry of the B_3 triangle and the locations of the hydrogen atoms relative to those seen in all other $B_3H_8^-$ anions.

Synthesis and Characterization of $Cp^*_2Co_2(B_6H_{14})$. Treatment of the cobalt(II) complex $[Cp^*CoCl]_2$ with NaB_3H_8 in diethyl ether, followed by pentane extraction and crystallization at −20 °C, affords light brown needles of $Cp^*_2Co_2(B_6H_{14})$ (**3**).

$$[Cp^*CoCl]_2 + 2\ NaB_3H_8 \rightarrow Cp^*_2Co_2(B_6H_{14}) + 2\ NaCl + H_2 \quad (3)$$

The spectroscopic characterization of **3** is best discussed after presenting the results of the crystallographic investigation; crystal data and important bond distances and angles for **3** are given in Tables 1 and 4. Molecules of **3** (Figure 3) reside on crystallographic 2-fold axes, and the two cobalt atoms are symmetry-related. The structure of **3** can be described in terms of an eight-vertex framework in which two Cp*Co fragments cap the same side of a somewhat helical B_6H_{14} chain. The B−B distances within the chain are as follows: B(3)−B(2) = 1.889(6), B(2)−B(1) = 1.809(6), and B(1)−B(1)′ = 1.734(8) Å; the latter B−B bond is the shortest by nearly 0.15 Å and, as we will show below, the only one not bridged by a hydrogen atom. The B−B−B angles in the B_6H_{14} chain are 111.2(3)° for B(1)−B(2)−B(3) and 118.2(3)° for B(2)−B(1)−B(1)′; these values are similar to those found in structurally similar "borallyl" complexes (see below). Each cobalt atom forms contacts with four of the six boron atoms in the chain, sharing the central B(1)−B(1)′ bond. The four Co−B distances in **3** are 2.157(5), 2.008(5), and 2.088(4) Å for boron atoms B(3), B(2), and B(1), respectively, where B(3) denotes the end of the chain. As we will show below, B(3) is involved in a Co−H−B bridging interaction. In contrast to the distribution of Co−B distances in **3**, which vary by 0.15 Å, the Co−B distances in Cp*Co(B_4H_{10}), which contains a structurally similar five-vertex core, are all about the same at 2.019 Å.[19]

All 14 of the boron-bound hydrogen atoms were apparent in the difference maps. The distribution of the 10 terminal hydrogen atoms along the B_6H_{14} chain is $H_3B-BH-BH-BH-BH-BH_3$, and the other four hydrogen atoms are bridging, one for each B−B bond except the central one. The average B−H bond distance for the terminal hydrogen atoms is 1.12(7) Å, and the average B−H bond distance for the B−H−B bridges is 1.27(7) Å. Of the three hydrogen atoms on each terminal boron atom, one bridges to cobalt, forming a Co−H distance of 1.48(3) Å; the B−H distance in each of these Co−H−B units is 1.28(3) Å.

Several other cobaltaborane molecules containing CpCo or Cp*Co fragments have been reported.[19−26] For example, Fehlner

Table 4. Important Bond Lengths (Å) and Angles (deg) for $Cp^*_2Co_2(B_6H_{14})$ (**3**)[a]

Bond Lengths (Å)			
Co(1)−B(1)	2.088(4)	B(1)−H(1)	1.07(3)
Co(1)−B(2)	2.008(5)	B(1)−H(12)	1.26(3)
Co(1)−B(3)	2.157(5)	B(2)−H(12)	1.29(3)
Co(1)−B(1)′	2.183(4)	B(2)−H(2)	1.15(3)
Co(1)′−(B1)	2.183(4)	B(2)−H(23)	1.20(3)
Co(1)−H(3C)	1.48(3)	B(3)−H(23)	1.34(4)
B(1)−B(2)	1.809(6)	B(3)−H(3A)	1.19(3)
B(2)−B(3)	1.889(6)	B(3)−H(3B)	1.08(3)
B(1)−B(1)′	1.734(8)	B(3)−H(3C)	1.28(3)
Bond Angles (deg)			
B(2)−Co(1)−B(1)	52.37(17)	Co(1)′−B(1)−H(12)	90.2(15)
B(2)−Co(1)−B(3)	53.79(18)	H(1)−B(1)−H(12)	109(2)
B(1)−Co(1)−B(3)	91.86(18)	B(1)−B(2)−B(3)	111.2(3)
B(2)−Co(1)−B(1)′	92.93(17)	B(1)−B(2)−Co(1)	66.1(2)
B(1)−Co(1)−B(1)′	47.8(2)	B(3)−B(2)−Co(1)	67.2(2)
B(3)−Co(1)−B(1)′	100.30(19)	B(1)−B(2)−H(12)	43.9(14)
B(2)−Co(1)−H(3C)	84.0(12)	B(3)−B(2)−H(12)	114.3(14)
B(1)−Co(1)−H(3C)	100.0(12)	Co(1)−B(2)−H(12)	106.4(14)
B(3)−Co(1)−H(3C)	35.5(12)	B(1)−B(2)−H(2)	120.7(14)
B(1)′−Co(1)−H(3C)	80.6(11)	B(3)−B(2)−H(2)	124.7(13)
B(1)′−B(1)−B(2)	118.2(3)	Co(1)−B(2)−H(2)	117.3(16)
B(1)′−B(1)−Co(1)	68.9(3)	H(12)−B(2)−H(2)	115.8(19)
B(2)−B(1)−Co(1)	61.5(2)	B(1)−B(2)−H(23)	118.2(15)
B(1)′−B(1)−Co(1)′	63.2(2)	B(3)−B(2)−H(23)	45.0(17)
B(2)−B(1)−Co(1)′	129.8(3)	Co(1)−B(2)−H(23)	109.7(17)
Co(1)−B(1)−Co(1)′	128.7(2)	H(12)−B(2)−H(23)	89.1(19)
B(1)′−B(1)−H(1)	122.8(15)	H(2)−B(2)−H(23)	115(2)
B(2)−B(1)−H(1)	110.7(14)	B(2)−B(3)−Co(1)	59.1(2)
Co(1)−B(1)−H(1)	115.2(15)	B(2)−B(3)−H(23)	39.0(15)
Co(1)′−B(1)−H(1)	105.5(14)	Co(1)−B(3)−H(23)	96.2(15)
B(1)′−B(1)−H(12)	125.8(14)	B(2)−B(3)−H(3A)	123.0(16)
B(2)−B(1)−H(12)	45.7(14)	Co(1)−B(3)−H(3A)	129.2(16)
Co(1)−B(1)−H(12)	103.6(15)		

[a] Symmetry transformations used to generate equivalent atoms: ′ = $y + 1, x - 1, -z$.

(15) Guggenberger, L. J. *Inorg. Chem.* **1970**, *9*, 367−373.
(16) Bishop, V. L.; Kodama, G. *Inorg. Chem.* **1981**, *20*, 2724−2727.
(17) Glore, J. D.; Rathke, J. W.; Schaeffer, R. *Inorg. Chem.* **1973**, *12*, 2175−2178.
(18) Nordman, C. E.; Reimann, C. *J. Am. Chem. Soc.* **1959**, *81*, 3538−3543.
(19) Nishihara, Y.; Deck, K. J.; Shang, M.; Fehlner, T. P.; Haggerty, B. S.; Rheingold, A. L. *Organometallics* **1994**, *13*, 4510−4522.
(20) Pipal, J. R.; Grimes, R. N. *Inorg. Chem.* **1979**, *18*, 257−263.
(21) Deck, K. J.; Fehlner, T. P.; Rheingold, A. L. *Inorg. Chem.* **1993**, *32*, 2794−2795.

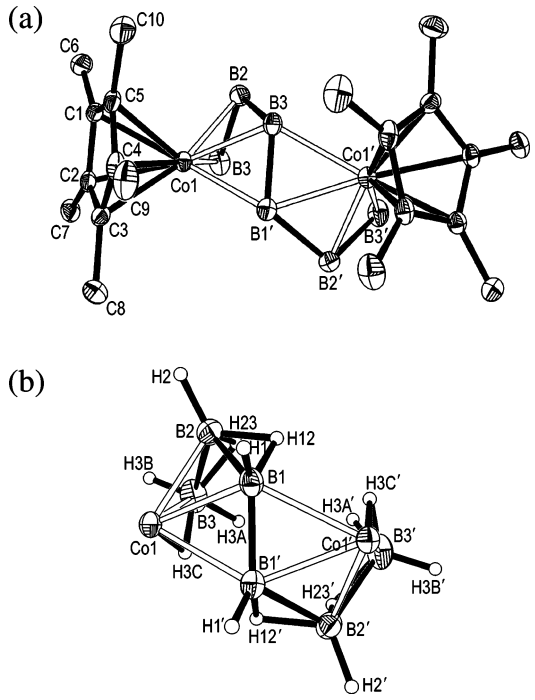

Figure 3. (a) Molecular structure of $Cp^*_2Co_2(B_6H_{14})$, **3**. Ellipsoids are drawn at the 35% probability level, except for hydrogen atoms, which are represented as arbitrarily sized spheres. All the hydrogen atoms have been deleted for clarity. (b) View of **3** showing hydrogen atoms in the B_6H_{14} unit. The Cp* groups have been deleted for clarity.

has prepared $Cp^*Co(B_4H_{10})$, $Cp^*_2Co_2(B_3H_7)$, and $Cp^*(Cp^*H)Co_2(B_3H_8)$ by treating $[Cp^*CoCl]_2$ with BH_3·THF and has isolated additional compounds—$Cp^*_2Co_2(B_2H_6)$, $Cp^*_3Co_3(B_2H_4)$, $Cp^*_3Co_3(B_3H_5)$, and $Cp^*_4Co_4(B_2H_4)$—by treating $[Cp^*CoCl]_2$ with $LiBH_4$.[19] Of these molecules, only $Cp^*Co(B_4H_{10})$ has an inner five-vertex CoB_4 core similar to that in **3**.

The ^1H and ^{11}B NMR spectra of **3** have been assigned with the assistance of selective and broad band $^1H\{^{11}B\}$ decoupled spectra and a two-dimensional [^1H,^{11}B] HMQC spectrum. The ^{11}B NMR spectrum exhibits three multiplets, all of which collapse to singlets of equal intensity in the $^{11}B\{^1H\}$ NMR spectrum. This spectrum is consistent with the presence of a B_6 ligand residing on a symmetry element that renders its two ends symmetry-equivalent. The ^1H NMR spectrum shows a singlet at δ 1.64 for the Cp* ligand; the B−H groups appear as several overlapping resonances between δ 4.0 and 0 and as three singlets at δ −3.32, −4.33, and −17.83 (Figure 4). The resonance at δ −17.83 is clearly due to the hydrogen atoms that bridge to cobalt, and the two resonances at δ −3.32 and −4.33 are due to BHB hydrogen atoms. In the $^1H\{^{11}B\}$ broad band decoupled spectrum, the complex pattern seen between δ 4.0 and 0 resolves into four singlets at 3.16, 2.66, 1.10, and 0.16, making seven different proton environments in all—each of intensity 2. Again, this finding is consistent with the 2-fold symmetry of the B_6H_{14} group. In the broad band decoupled $^1H\{^{11}B\}$ spectrum, the resonance at δ −17.83 is a doublet (J_{HH} = 27 Hz) owing to H−H coupling to the resonance at δ 0.16. The $^1H\{^{11}B\}$ selective decoupling experiments and the two-dimensional [^1H,^{11}B] HMQC spectrum (Figure 5) showed that the resonances at δ −17.83, 0.16, and 1.10 are assignable to the three terminal hydrogen atoms on B(3), the resonances at δ −4.33, −3.32, and 3.16 are assignable to protons attached to B(2), and the resonances at δ −3.32 and 2.66 are due to protons attached to B(1), the boron atom nearest to the middle of the

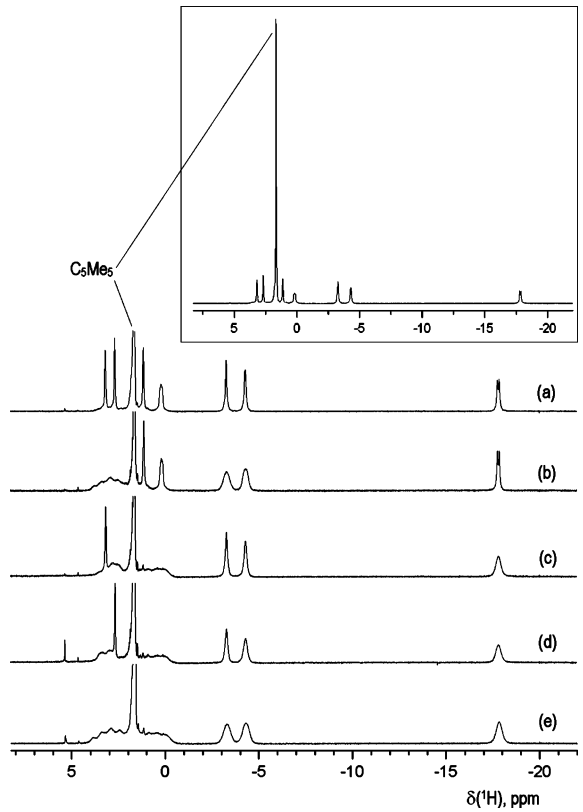

Figure 4. (a) Broad band decoupled $^1H\{^{11}B\}$ NMR spectrum of $Cp^*_2Co_2(B_6H_{14})$, **3**, in CD_2Cl_2 at 20 °C; (b) $^1H\{^{11}B\}$ NMR spectrum selectively decoupled at B3, (c) $^1H\{^{11}B\}$ NMR spectrum selectively decoupled at B2, (d) $^1H\{^{11}B\}$ NMR spectrum selectively decoupled at B1, (e) ^1H NMR spectrum.

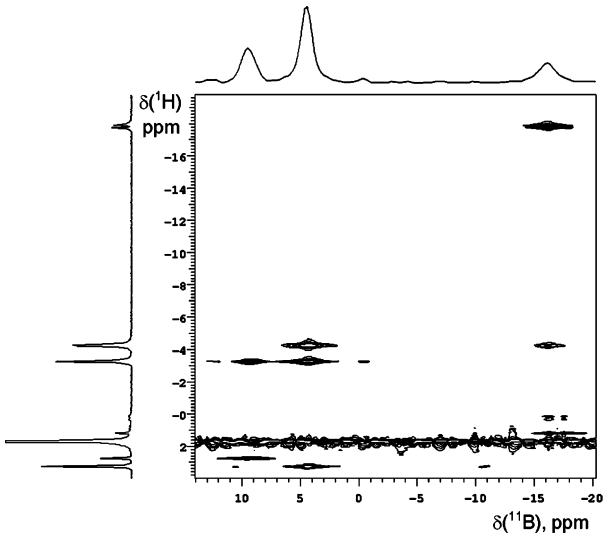

Figure 5. Two-dimensional [^1H,^{11}B] HMQC NMR spectrum of $Cp^*_2Co_2(B_6H_{14})$, **3**, in CD_2Cl_2 at 20 °C. Boron atoms B1, B2, and B3 resonate at δ 8.88, δ 3.78, and δ −16.42, respectively.

(22) Jiang, F.; Fehlner, T. P.; Rheingold, A. L. *J. Am. Chem. Soc.* **1987**, *109*, 1860−1861.
(23) Jiang, F.; Fehlner, T. P.; Rheingold, A. L. *J. Organomet. Chem.* **1988**, *348*, C22−C26.
(24) Jiang, F.; Fehlner, T. P.; Rheingold, A. L. *Angew. Chem., Int. Ed. Engl.* **1988**, *27*, 424−426.
(25) Micciche, R. P.; Carroll, P. J.; Sneddon, L. G. *Organometallics* **1985**, *4*, 1619−1623.
(26) Nishihara, Y.; Deck, K. J.; Shang, M.; Fehlner, T. P. *J. Am. Chem. Soc.* **1993**, *115*, 12224−12225.

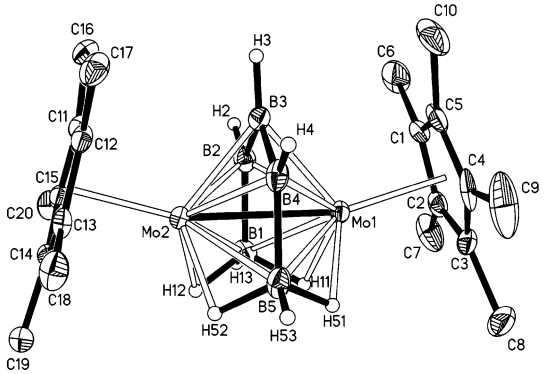

Figure 6. Molecular structure of $Cp^*_2Mo_2(B_5H_9)$, **2**. Ellipsoids are drawn at the 35% probability level, except for hydrogen atoms, which are represented as arbitrarily sized spheres. Methyl hydrogen atoms in the Cp* group have been deleted for clarity.

Table 5. Important Bond Lengths (Å) and Angles (deg) for $Cp^*_2Mo_2(B_5H_9)$ (**4**)

Bond Lengths (Å)			
Mo(1)−Mo(2)	2.8085(6)	Mo(2)−B(5)	2.312(4)
Mo(1)−H(11)	1.79(3)	B(1)−B(2)	1.732(6)
Mo(1)−H(51)	1.82(4)	B(2)−B(3)	1.715(6)
Mo(2)−H(12)	1.88(3)	B(3)−B(4)	1.712(7)
Mo(2)−H(52)	1.85(3)	B(4)−B(5)	1.735(7)
Mo(1)−B(1)	2.320(4)	B(1)−H(11)	1.268(18)
Mo(1)−B(2)	2.213(4)	B(1)−H(12)	1.272(18)
Mo(1)−B(3)	2.181(4)	B(1)−H(13)	1.06(3)
Mo(1)−B(4)	2.208(4)	B(2)−H(2)	1.07(2)
Mo(1)−B(5)	2.322(4)	B(3)−H(3)	1.07(2)
Mo(2)−B(1)	2.323(4)	B(4)−H(4)	1.07(2)
Mo(2)−B(2)	2.211(4)	B(5)−H(51)	1.274(18)
Mo(2)−B(3)	2.175(4)	B(5)−H(52)	1.272(18)
Mo(2)−B(4)	2.216(4)	B(5)−H(53)	1.06(3)
Bond Angles (deg)			
B(3)−B(2)−B(1)	123.2(3)	Mo(1)−B(1)−Mo(2)	74.45(12)
B(3)−B(4)−B(5)	122.9(3)	Mo(1)−B(4)−Mo(2)	78.83(14)
B(4)−B(3)−B(2)	121.5(3)	Mo(2)−B(2)−Mo(1)	78.83(14)
H(11)−Mo(1)−H(51)	68.5(15)	Mo(2)−B(3)−Mo(1)	80.30(14)
H(12)−Mo(2)−H(52)	68.6(13)	Mo(2)−B(5)−Mo(1)	74.62(13)

six-atom chain. From these data, and by taking the resonance at δ −17.84 to be due to the Co−H−B bridging hydrogen atom, the other proton resonances can easily be assigned (Figure 4). The variable temperature $^1H\{^{11}B\}$ NMR spectrum between −80 and 20 °C shows no evidence of fluxionality.

Synthesis and Characterization of $Cp^*_2Mo_2(B_5H_9)$. Treatment of the molybdenum(III) complex $[Cp^*MoCl_2]_2$ with NaB_3H_8 in THF, followed by pentane extraction and crystallization at −20 °C, affords red−orange crystals of $Cp^*_2Mo_2(B_5H_9)$ (**4**).

$$[Cp^*MoCl_2]_2 + 4\ NaB_3H_8 \rightarrow Cp^*_2Mo_2(B_5H_9) + \ldots \quad (4)$$

Compound **4** has previously been obtained from the reaction of $[Cp^*MoCl_2]_2$ or Cp^*MoCl_4 with BH_3·THF.[27,28] The molecular structure of **4** (which had not previously been determined) is shown in Figure 6. Crystal data and important bond distances and angles for **4** are given in Tables 1 and 5. The structure of **4** closely resembles those of $Cp^*_2Cr_2(B_5H_9)$,[27] $(C_5H_4Me)_2Mo_2(B_5H_9)$,[29] and $Cp^*_2W_2(B_5H_9)$:[30] the five boron atoms form a planar C-shaped unit, capped on each side by a Cp*Mo unit. The structure of **4** can also be viewed as a bicapped trigonal bipyramid in which B(3), Mo(1), and Mo(2) occupy the equatorial positions and two BH_3 fragments cap the Mo(1)−B(2)−Mo(2) and Mo(1)−B(4)−Mo(2) faces of the Mo_2B_3 skeleton.

All of the boron-bound hydrogen atoms are terminal with respect to boron, and their distribution within the B_5H_9 chain is $H_3B-BH-BH-BH-BH_3$. Of the three H atoms on each BH_3 unit, one bridges to one Mo atom, one bridges to the other Mo atom, and the third H atom is strictly terminal on boron. All the bond lengths and bond angles in **4** are very similar to those in the $(C_5H_4Me)_2Mo_2(B_5H_9)$ analogue.[29] The Mo−Mo distance is 2.8085(6) Å, and the Mo−H distances for the Mo−H−B bridges average 1.83(3) Å. The average B−H distance within the Mo−H−B bridges is 1.27(2) Å, and the average B−H distance for the terminal hydrogen atoms is 1.07(2) Å. The B(1)−B(2) and B(4)−B(5) distances (at the ends of the B5 chain) of 1.73(1) Å are equal within experimental error and are longer than the two other chemically equivalent B(2)−B(3) and B(3)−B(4) edges by about 0.02 Å.

The $^{11}B\{^1H\}$ NMR spectrum matches that previously reported by Fehlner[28] and closely resembles that of the C_5H_4Me analogue described by Green.[29] For reasons we do not understand (i.e., despite the use of the same solvent), the ^1H NMR chemical shifts for the BH groups previously reported[28] for **4** differ from those we find by about 0.4 ppm. Our assignments of the ^1H NMR spectrum, as deduced from a series of $^1H\{$selective-$^{11}B\}$ NMR spectra, correspond to those made by Green: the doublet at δ −6.84 is due to the Mo−H−B hydrogen atoms on B(1) and B(5); the triplet at δ 5.61 is due to the protons attached to B(2) and B(4); the triplet at δ 5.01 is due to the BH terminal hydrogen atoms on B(1) and B(5); and the triplet at δ 3.43 is due to the proton on B(3).

Discussion

Comparison of the Structures of $Cp^*M(B_3H_8)_2$ Complexes. The compounds $Cp^*V(B_3H_8)_2$ (**1**) and $Cp^*Cr(B_3H_8)_2$ (**2**) have the same ligand sets: one Cp* ligand and two B_3H_8 groups. Their molecular structures, however, differ significantly; the vanadium compound contains two bidentate B_3H_8 ligands (i.e., bound via two vicinal hydrogen atoms), whereas the chromium compound has one bidentate B_3H_8 ligand and one B_3H_8 ligand bound in a very different way. Specifically, the second B_3H_8 ligand in **2** coordinates to the chromium center via two *geminal* hydrogen atoms. This is the first example in any transition metal complex of such a gem-bound B_3H_8 coordination mode. The nearest analogue was described in a computational study of the dynamics of $[CuCl(B_3H_8)]^-$,[31] in which a similar gem-bound B_3H_8 structure was proposed as an intermediate in the fluxional exchange pathway for the B_3H_8 ligand.

We now turn to the question of why $Cp^*V(B_3H_8)_2$ (**1**) and $Cp^*Cr(B_3H_8)_2$ (**2**) adopt different structures. We propose that the different B_3H_8 coordination modes in **1** and **2** can be explained in terms of number of empty valence orbitals on the metal centers: seven for d^2 vanadium(III) and six for d^3

(27) Aldridge, S.; Fehlner, T. P.; Shang, M. Y. *J. Am. Chem. Soc.* **1997**, *119*, 2339−2340.
(28) Aldridge, S.; Shang, M. Y.; Fehlner, T. P. *J. Am. Chem. Soc.* **1998**, *120*, 2586−2598.
(29) Bullick, H. J.; Grebenik, P. D.; Green, M. L. H.; Hughes, A. K.; Leach, J. B.; McGowan, P. C. *J. Chem. Soc., Dalton Trans.* **1995**, 67−75.
(30) Weller, A. S.; Shang, M. Y.; Fehlner, T. P. *Organometallics* **1999**, *18*, 53−64.
(31) Serrar, C.; Es-sofi, A.; Boutalib, A.; Quassas, A.; Jarid, A.; Nebot-Gil, I.; Tomas, F. *J. Phys. Chem. A* **2001**, *105*, 9776−9780.

chromium(III). On each metal center, three of these empty orbitals are involved in metal−Cp* bonding, leaving four and three orbitals for metal−B_3H_8 bonding, respectively. The usual bidentate B_3H_8 binding mode involving two mutually *vicinal* hydrogen atoms requires two empty metal orbitals, whereas the new B_3H_8 binding mode involving two *geminal* hydrogen atoms must only require one empty metal orbital. Thus, Cp*V$(B_3H_8)_2$ with four empty orbitals has two bidentate B_3H_8 ligands, whereas Cp*Cr$(B_3H_8)_2$ with three empty orbitals has one bidentate and one gem-bound B_3H_8 group, the latter behaving in an electronic sense like a "pseudo-unidentate" ligand.

Steric factors also favor the observed difference in the geometries of **1** and **2**. Comparisons of the metal−ligand distances in Cp*V$(B_3H_8)_2$ with those in Cp*Cr$(B_3H_8)_2$ suggest (as expected) that the radius of V^{III} is roughly 0.15 Å larger than that of Cr^{III}. Thus, the vanadium compound **1** is expected to favor higher hapticities for the B_3H_8 groups, as is observed.

Bonding in the Unusual Cobaltaborane Cluster Cp*$_2$Co$_2$(B_6H_{14}). The structure of Cp*$_2$Co$_2$(B_6H_{14}) (**3**) can be viewed in two different ways: as a dicobalt complex in which two Cp*Co units are bound to the B_6H_{14} ligand, or as an eight-vertex *hypho* cluster compound. We will discuss these alternatives in turn.

There are two ways in which the B_6H_{14} group in **3** can be regarded: (a) as a neutral unit isoelectronic with 1,3,5-hexatriene (C_6H_8), or (b) as a dianion ($B_6H_{14}^{2-}$) isoelectronic with a diallylic hexadienediyl dianion ($C_6H_8^{2-}$):

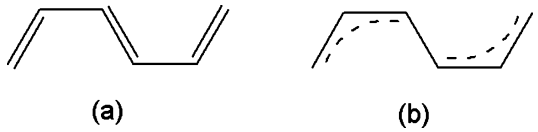

These alternatives can be distinguished by comparison with known complexes containing hexatriene (or hexadienediyl) ligands. In only a few cases is the C_6H_8 ligand best regarded as a neutral triene, one example being the cluster $Ru_6(CO)_{14}$(μ-C)(*trans*-1,3,5-hexatriene).[32] In this molecule, two ruthenium centers are bound to the hextatriene group in a η^4,η^2 fashion—that is, unsymmetrically. The C−C bond distances alternate down the chain between short and long bonds, as expected for a neutral 1,3,5-hexatriene. Neither the unsymmetric binding mode nor the pattern of bond distances within the chain resemble the structural features seen in **3**.

Diallylic hexadienediyl species are somewhat more common. In the lithium salt [Li(tmed)]$_2$[C_6H_8],[33] where tmed = *N*,*N*,*N*′,*N*′-tetramethylethylenediamine, each lithium atom interacts with four of the carbon atoms, with the longest Li−C contacts being to the two central carbon atoms. Except for the central C−C bond, all the C−C bond distances are nearly identical. All of these structural features closely resemble those seen in **3**. One difference is that the central C−C bond in this organic dianion is longer than the other bonds, whereas the central B−B bond in **3** is shorter than the others. Most likely, this difference reflects the fact that only the central B−B bond in **3** is not hydrogen-bridged. One other minor difference is that the C_6H_8 dianion usually adopts an s-*trans*, s-*trans* conformation rather than the s-*cis*, s-*cis* conformation seen in **3**.

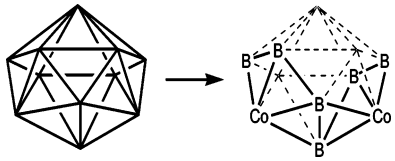

Figure 7. A schematic drawing showing the construction of the eight-vertex *hypho* cluster of Cp*$_2$Co$_2$(B_6H_{14}), **3** (right), from the eleven-vertex *closo* octadecahedron (left).

The B_6H_{14} ligand in **3** may also be compared with complexes of the heptahydrotriborate dianion, $B_3H_7^{2-}$, which has been termed a "borallyl" ligand because it is isoelectronic with and structurally analogous to the allyl ligand, $C_3H_5^-$. Borallyl complexes are known for several transition metals, including Co,[34] Ir,[35−37] Pd,[38,39] and Pt.[40−42] The bond distances and angles that describe the Co−B_6H_{14} interactions in **3** are very similar to those seen in complexes of the B_3H_7 ligand, and **3** can be regarded as a cobalt complex of the previously unknown biborallyl dianion.

The above bonding analysis treated the B_6H_{14} unit as a ligand to two separate cobalt centers; it is also useful to analyze it from a cluster point of view and to regard the B_6H_{14} unit as a component of a cluster framework. The total cluster valence electron count for Cp*$_2$Co$_2$(B_6H_{14}) is 60; subtracting 20 electrons for the d-orbital "sinks" on the two cobalt centers leaves a bonding electron count of 40 for this eight-vertex polyhedron. According to cluster electron counting rules, the cluster is therefore a member of the eight-vertex *hypho* class. An eight-vertex *hypho* cluster should be obtainable by removing three adjacent high-connectivity vertices from the eleven-vertex *closo* polyhedron, which is an octadecahedron. In fact, the structure of **3** is exactly that (Figure 7). The locations of the cobalt atoms within the *hypho* framework are consistent with the predictions of the Wade−Mingos theory:[43] because the cobalt atoms are larger than boron, they occupy the vertices in the *hypho* framework that have the highest connectivities.

Several other eight-vertex boron-containing *hypho* clusters are known; among these are [$C_2B_6H_{13}^-$],[44] $C_2B_6H_{11}R(PHPh_2)$ (R = H or Me),[45] $NCB_6H_{11}Me$,[46] [$S_2B_6H_9^-$],[47] $S_2B_6H_8Me_2$,[47] NSB_6H_{11},[48] and [$CSB_6H_{11}^-$].[49] In all of these compounds, the two heteroatoms (carbon, nitrogen, or sulfur) bridge nonadjacent edges of a pentagonal pyramidal B_6 subunit, and the eight-vertex

(32) Adams, R. D.; Wu, W. G. *Organometallics* **1993**, *12*, 1243−1247.
(33) Arora, S. K.; Bates, R. B.; Beavers, W. A.; Cutler, R. S. *J. Am. Chem. Soc.* **1975**, *97*, 6271−6272.
(34) Lei, X. J.; Shang, M. Y.; Fehlner, T. P. *Organometallics* **1998**, *17*, 1558−1563.
(35) Greenwood, N. N.; Kennedy, J. D.; Reed, D. *J. Chem. Soc., Dalton Trans.* **1980**, 196−200.
(36) Bould, J.; Greenwood, N. N.; Kennedy, J. D.; McDonald, W. S. *J. Chem. Soc., Dalton Trans.* **1985**, 1843−1847.
(37) Lei, X. J.; Bandyopadhyay, A. K.; Shang, M. Y.; Fehlner, T. P. *Organometallics* **1999**, *18*, 2294−2296.
(38) Housecroft, C. E.; Owen, S. M.; Raithby, P. R.; Shaykh, B. A. M. *Organometallics* **1990**, *9*, 1617−1623.
(39) Housecroft, C. E.; Shaykh, B. A. M.; Rheingold, A. L.; Haggerty, B. S. *Inorg. Chem.* **1991**, *30*, 125−130.
(40) Bould, J.; Kennedy, J. D.; McDonald, W. S. *Inorg. Chim. Acta* **1992**, *196*, 201−208.
(41) Guggenberger, L. J.; Kane, A. R.; Muetterties, E. L. *J. Am. Chem. Soc.* **1972**, *94*, 5665−5673.
(42) Haggerty, B. S.; Housecroft, C. E.; Rheingold, A. L.; Shaykh, B. A. M. *J. Chem. Soc., Dalton Trans.* **1991**, 2175−2184.
(43) Jemmis, E. D.; Balakrishnarajan, M. M.; Pancharatna, P. D. *Chem. Rev.* **2002**, *102*, 93−144 and references therein.
(44) Jelinek, T.; Holub, J.; Stibr, B.; Fontaine, X. L. R.; Kennedy, J. D. *Collect. Czech. Chem. Commun.* **1994**, *59*, 1584−1595.
(45) Hong, D.; Carroll, P. J.; Sneddon, L. G. *Organometallics* **2004**, *23*, 711−717.
(46) Jelinek, T.; Stibr, B.; Kennedy, J. D.; Hnyk, D.; Buhl, M.; Hofmann, M. *J. Chem. Soc., Dalton Trans.* **2003**, 1326−1331.
(47) Kang, S. O.; Sneddon, L. G. *J. Am. Chem. Soc.* **1989**, *111*, 3281−3289.

hypho frameworks are constructed by removing three *mutually* adjacent high-connectivity vertices of the parent eleven-vertex *closo* polyhedron, the octadecahedron. In contrast, the framework seen for **3** is generated by removing three vertices that are not all mutually adjacent. Several clusters of formula B_8H_{11}(NHR)(L) are also known that can be regarded either as eight-vertex *hypho* clusters or as nine-vertex *arachno* clusters.[50−52] To our knowledge, compound **3** is the first eight-vertex *hypho* metallaborane cluster.

Experimental Section

All experiments were carried out under vacuum or under argon by using standard Schlenk techniques. Solvents were distilled under nitrogen from sodium/benzophenone immediately before use. The starting materials NaB_3H_8,[53] $[Cp^*VCl_2]_3$,[54] $[Cp^*CrCl_2]_2$,[55] $[Cp^*CoCl]_2$,[56,57] and $[Cp^*MoCl_2]_2$[58] were prepared by literature procedures. Microanalyses were performed by the University of Illinois Microanalytical Laboratory. The IR spectra were recorded on a Nicolet Impact 410 instrument as Nujol mulls. The ^{1}H and ^{11}B NMR data were collected on a wide bore instrument at 300.102 and 96.285 MHz, respectively. Chemical shifts are reported in δ units (positive shifts to high frequency) relative to tetramethylsilane (^{1}H NMR) or $BF_3{\cdot}Et_2O$ (^{11}B NMR). Magnetic moments were determined in C_6D_6 by the Evans NMR method on a Varian Gemini 500 instrument at 499.699 MHz.

Caution. NaB_3H_8 and its compounds are often pyrophoric. They should be handled with strict exclusion of air and moisture in a well-ventilated fume hood.

Bis(octahydrotriborato)(pentamethylcyclopentadienyl)vanadium(III), $Cp^*V(B_3H_8)_2$, 1. To a suspension of $[Cp^*VCl_2]_3$ (0.47 g, 0.61 mmol) in diethyl ether (20 mL) at −78 °C was added a solution of NaB_3H_8 (0.26 g, 4.1 mmol) in diethyl ether (20 mL). The reaction mixture was stirred at −78 °C for 30 min and was allowed to warm to room temperature and stirred for 7 h. The solution color changed from purple to green, and a white precipitate formed. The green solution was filtered, concentrated to ca. 15 mL, and cooled to −20 °C to afford light green crystals. Yield: 0.40 g (82%). Single crystals for the X-ray diffraction experiment were obtained by recrystallization from pentane solution. The product can also be isolated by sublimation at 70 °C and 0.05 Torr with slight decomposition. FD-MS *m*/*z* 267.2 (M^+). Anal. Calcd for $C_{15}H_{31}B_6V$: C, 45.0; H, 11.7; B, 19.1; V, 24.3. Found: C, 43.4; H, 11.0; B, 19.4; V, 24.4. ^{1}H NMR (C_6D_6, 20 °C): δ −13.8 (s, fwhm = 2250 Hz, Cp*). Magnetic moment (C_6D_6, 20 °C): 2.7 μ_B. IR (cm^{-1}): 2517 s, 2467 s, 2364 sh, 2283 w, 2131 s, 2082 s, 2044 s, 1424 m, 1307 s, 1183 w, 1145 w, 1070 w, 1044 s, 1021 s, 977 s, 873 m, 844 s, 803 w, 780 w, 653 m, 619 w.

Bis(octahydrotriborato)(pentamethylcyclopentadienyl)chromium(III), $Cp^*Cr(B_3H_8)_2$, 2. To a solution of $[Cp^*CrCl_2]_2$ (0.084 g, 0.16 mmol) in diethyl ether (20 mL) at 0 °C was added a solution of NaB_3H_8 (0.050 g, 0.79 mmol) in diethyl ether (15 mL). The reaction mixture was stirred at 0 °C for 30 min and was allowed to warm to room temperature. After the mixture had been stirred for 8 h, the blue−green solution was filtered, and the solvent was removed in vacuum. The residue was extracted with pentane (35 mL), and the pentane extract was filtered and concentrated to 10 mL. Crystallization at −20 °C afforded dark green crystals. Yield: 0.038 g (43%). Anal. Calcd for $C_{15}H_{31}B_6Cr$: C, 44.8; H, 11.7. Found: C, 44.8; H, 10.7. ^{1}H NMR (C_6D_6, 20 °C): δ −74.4 (s, fwhm = 900 Hz, Cp*). Magnetic moment (C_6D_6, 20 °C): 4.1 μ_B. IR (cm^{-1}): 2514 sh, 2482 s, 2456 s, 2418 s, 2303 w, 2281 w, 2094 s, 2002 sh, 1308 s, 1262 sh 1147 s, 1102 m, 1072 m, 1018 s, 976 s, 872 m, 844 m, 802 w, 748 w, 655 m, 583 w, 514 w, 448 s.

(Tetradecahydrohexaborato)bis(pentamethylcyclopentadienyl)dicobalt, $Cp^*_2Co_2(B_6H_{14})$, 3. To a solution of $[Cp^*CoCl]_2$ (0.96 g, 2.1 mmol) in diethyl ether (25 mL) at −78 °C was added a solution of NaB_3H_8 (0.30 g, 4.7 mmol) in diethyl ether (25 mL). The reaction mixture was stirred at −78 °C for 30 min and then allowed to warm slowly to room temperature. Gas slowly evolved. The mixture was stirred at room temperature for 8 h to give a dark red solution and a pale green precipitate. The dark red solution was filtered, and the solvent was removed under vacuum. The brown residue was extracted with pentane (50 mL), and the extract was filtered and cooled to −78 °C to afford brown−red needles. Yield: 0.39 g (40%). Single crystals for X-ray diffraction were grown at −20 °C. Anal. Calcd for $C_{20}H_{44}B_6Co_2$: C, 51.4; H, 9.49; B, 13.9; Co, 25.2. Found: C, 50.8; H, 9.20; B, 14.4, Co, 25.7. ^{1}H{^{11}B} NMR (CD_2Cl_2, 20 °C): δ 3.16 (s, 2H, BH), 2.66 (s, 2H, BH), 1.64 (s, 30H, C_5Me_5), 1.10 (s, 2H, BH_2), 0.16 (s, 2H, BH_2), −3.32 (s, 2H, BHB), −4.33 (s, 2H, BHB), −17.83 (d, J_{HH} = 27 Hz, 2H, CoHB). ^{11}B{^{1}H} NMR (CD_2Cl_2, 20 °C): δ 8.88 (s, 2B), 3.78 (s, 2B), −16.42 (s, 2B). IR (cm^{-1}): 2521 s, 2480 s, 2413 s, 2362 m, 1894 m, 1826 s, 1155 vs, 1060 m, 1040 w, 1022 vs, 950 vs, 909 m, 875 m, 797 s, 652 w, 600 w.

(Nonahydropentaborato)bis(pentamethylcyclopentadienyl)dimolybdenum, $Cp^*_2Mo_2(B_5H_9)$, 4. To a solution of $[Cp^*MoCl_2]_2$ (0.38 g, 0.63 mmol) in tetrahydrofuran (10 mL) was added a solution of NaB_3H_8 (0.16 g, 2.7 mmol) in THF (20 mL). Gas slowly evolved. The reaction mixture was stirred at room temperature for 6 days to give red solution and white precipitate. The red solution was filtered, and the solvent was removed in vacuum. The red residue was extracted with pentane (40 mL), and the extract was filtered and concentrated to 10 mL. Crystallization at −20 °C afforded red−orange crystals. Yield: 0.06 g (18%). ^{1}H{^{11}B} NMR (C_6D_6, 20 °C): δ 5.61 (t, J_{HH} = 4.8 Hz, 2H, BH), 5.01 (t, J_{HH} = 12.3 Hz, 2H, BH), 3.43 (t, J_{HH} = 5.4 Hz, 1H, BH), 1.93 (s, 30H, C_5Me_5), −6.84 (d, J_{HH} = 13.5 Hz, 4H, MoHB). ^{11}B{^{1}H} NMR (C_6D_6, 20 °C): δ 65.6 (s, 3B), 28.4 (s, 2B).

X-ray Structure Determinations.[59] Single crystals of all three compounds, grown from pentane, were mounted on glass fibers with Paratone-N oil (Exxon) and immediately cooled to −80 °C in a cold nitrogen gas stream on the diffractometer. Standard peak search and indexing procedures gave rough cell dimensions. Data for **1**−**4** were collected with an area detector by using the measurement parameters listed in Table 1. The measured intensities were reduced to structure factor amplitudes and their estimated standard deviations by correction for background and Lorentz and polarization effects. Systematically absent reflections were deleted and symmetry-equivalent reflections were averaged to yield the sets of unique data. The analytical approximations to the scattering factors were used, and all structure factors were corrected for both real and imaginary components of anomalous dispersion. All structures were solved using direct methods (SHELXTL). The correct positions for all non-hydrogen atoms of **1**−**4** were deduced from E-maps. Methyl hydrogen atoms were placed in idealized positions with C−H = 0.98 Å, and their displacement

(48) Jelinek, T.; Kennedy, J. D.; Stibr, B. *J. Chem. Soc., Chem. Commun.* **1993**, 1628−1629.
(49) Holub, J.; Kennedy, J. D.; Jelinek, T.; Stibr, B. *J. Chem. Soc., Dalton Trans.* **1994**, 1317−1323.
(50) MacKinnon, P.; Fontaine, X. L. R.; Kennedy, J. D.; Salter, P. A. *Collect. Czech. Chem. Commun.* **1996**, *61*, 1773−1782.
(51) Dorfler, U.; Bauer, C.; Gabel, D.; Rath, N. P.; Barton, L.; Kennedy, J. D. *J. Organomet. Chem.* **2000**, *614*, 215−222.
(52) Bauer, C.; Gabel, D.; Borrmann, T.; Kennedy, J. D.; Kilner, C. A.; Thornton-Pett, M.; Dorfler, U. *J. Organomet. Chem.* **2002**, *657*, 205−216.
(53) Hough, W. V.; Edwards, L. J.; McElroy, A. D. *J. Am. Chem. Soc.* **1958**, *80*, 1828−1829.
(54) Abernethy, C. D.; Bottomley, F.; Chen, J.; Kemp, M. F.; Mallais, T. C.; Womiloju, O. O. *Inorg. Synth.* **1998**, *32*, 207−214.
(55) Richeson, D. S.; Mitchell, J. F.; Theopold, K. H. *Organometallics* **1989**, *8*, 2570−2577.
(56) Kolle, U.; Khouzami, F.; Fuss, B. *Angew. Chem., Int. Ed. Engl.* **1982**, *21*, 131−132.
(57) Koelle, U.; Fuss, B.; Belting, M.; Raabe, E. *Organometallics* **1986**, *5*, 980−987.
(58) Abugideiri, F.; Brewer, G. A.; Desai, J. U.; Gordon, J. C.; Poli, R. *Inorg. Chem.* **1994**, *33*, 3745−3751.
(59) For details of the crystallographic methods used, see: Brumaghim, J. L.; Priepot, J, G.; Girolami, G. S. *Organometallics* **1999**, *18*, 2139−2144.

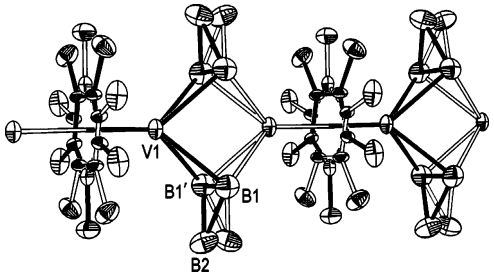

Figure 8. Drawing showing the disorder present in $Cp^*V(B_3H_8)_2$, **1**; all atoms have 50% site occupancy factors except for B1, which is 100% owing to the coincident coordinates of the disordered components. The disordered molecules are represented by black and white bonds, respectively. Thermal ellipsoids are drawn at the 35% probability level; hydrogen atoms are omitted for clarity.

parameters were set to equal to 1.5 times U_{eq} for the attached carbon. Final refinement parameters for **1**−**4** are given in Table 1. Subsequent discussions for **1**−**4** will be divided into individual paragraphs.

(a) $Cp^*V(B_3H_8)_2$, 1. Systematic absences for hkl ($h + k \neq 2n$) were consistent with space groups $C2$, Cm, and $C2/m$; the last of these was proven to be the correct choice by the success of the subsequent refinement. No corrections for absorption or crystal decay were applied. All atoms except B(1) were disordered over two sites; the symmetry elements require that the site occupancy factors for the disordered positions be exactly 50% (see below). Hydrogen atoms attached to boron were located in the difference maps, and their positions were refined with independent isotropic displacement parameters. The B−H distances to H(21) and H(22) were constrained to be equal within a standard deviation of 0.05 Å, as were the chemically related B−H distances to H(13) and H(14). The quantity minimized by the least-squares program was $\sum w(F_o^2 - F_c^2)^2$, where $w = \{[\sigma(F_o^2)]^2 + (0.0260P)^2 + 0.53P\}^{-1}$ and $P = (F_o^2 + 2F_c^2)/3$. The crystal used was evidently slightly twinned, with the twin law being reflection through the b^*c^* plane (i.e., a plane perpendicular to the a-axis); the volume fraction of the major twin individual refined to 0.960(4). Successful convergence was indicated by the maximum shift/error of 0.000 for the last cycle. Final refinement parameters are given in Table 1. The largest peak in the final Fourier difference map (0.21 eÅ^{-3}) was located 1.35 Å from H(6C). A final analysis of variance between observed and calculated structure factors showed no apparent errors.

The disorder in this crystal is unusual (Figure 8). The crystal structure consists of stacks of molecules running in linear chains parallel to the c-axis. Within each stack, each molecule is oriented identically with its Cp*−V axis collinear with the stacking axis (Cp* here standing for the centroid of the ring). There are two choices for the stacking order: the Cp*−V vector can be oriented with its Cp* end either toward the positive c-axis or toward the negative c-axis. From stack to stack, there is evidently no preference whether adjacent stacks will have their Cp*−V vectors oriented in the same direction or in opposite directions (no evidence of a supercell could be found in the diffraction record). This disorder causes the diffraction pattern to correspond to a structure in which the two types of chains are superimposed in the unit cell, each chain being constituted of atoms with site occupancies of 0.5. Thus, within each repeat unit of each chain, there are two half-Cp* rings (superimposed but staggered with respect to each other), two half-vanadium atoms (one on each side of the Cp* ring), and four half-occupancy B_3H_8 groups (of which the vanadium-bound boron atoms are almost exactly superimposed and treatable as full-occupancy atoms). A somewhat similar disorder is present in the crystal structure of Cp^*ReO_3.[60]

There are two choices to determine the boron atoms that form the B_3H_8 groups. We chose to match the B(1) atoms with the half-occupancy boron atom B(2), rather than its symmetry-related counterpart. This choice yields the most chemically reasonable dihedral angle of 119.7(5)° between the plane passing through three boron atoms in the B_3H_8 ligand, B(1)−B(1)′−B(2), and the plane passing through the metal center and two vanadium-bound boron atoms, V(1)−B(1)−B(1)′. Despite the disorder, the hydrogen atoms in the B_3H_8 groups were apparent in the difference maps and, after applying light constraints to the hydrogen atoms attached to B(2), correspond to chemically very reasonable positions.

(b) $Cp^*Cr(B_3H_8)_2$, 2. Systematic absences for $0kl$ ($k \neq 2n$), $h0l$ ($l \neq 2n$), and $hk0$ ($h + k \neq 2n$) were only consistent with the space group $Pbcn$. All 3199 data were used in the least-squares refinement. Although corrections for crystal decay were unnecessary, a face-indexed absorption correction was applied. The quantity minimized by the least-squares program was $\sum w(F_o^2 - F_c^2)^2$, where $w = \{[\sigma(F_o^2)]^2 + (0.0495P)^2\}^{-1}$ and $P = (F_o^2 + 2F_c^2)/3$. Hydrogen atoms attached to boron were easily located in the difference maps, and their positions were refined with independent isotropic displacement parameters. Successful convergence was indicated by the maximum shift/error of 0.000 for the last cycle. The largest peak in the final Fourier difference map (0.24 eÅ^{-3}) was located 0.73 Å from C(5). A final analysis of variance between observed and calculated structure factors showed no apparent errors.

(c) $Cp^*_2Co_2(B_6H_{14})$, 3. Systematic absences for $00l$ ($l \neq 4n$) and $h00$ ($h \neq 2n$) were consistent with space groups $P4_12_12$ and $P4_32_12$; the latter was chosen, but the data crystal proved to be an inversion twin in which the major twin individual had a volume fraction of 0.56(3). A total of 2272 unique data were used in the least-squares refinement. Although corrections for crystal decay were unnecessary, a face-indexed absorption correction was applied. No correction for isotropic extinction was necessary. Hydrogen atoms attached to boron were easily located in the difference maps, and their positions were refined with independent isotropic displacement parameters. The quantity minimized by the least-squares program was $\sum w(F_o^2 - F_c^2)^2$, where w $= \{[\sigma(F_o^2)]^2 + (0.0280P)^2\}^{-1}$ and $P = (F_o^2 + 2F_c^2)/3$. Successful convergence was indicated by the maximum shift/error of 0.000 for the last cycle. The largest peak in the final Fourier difference map (0.24 eÅ^{-3}) was located 0.83 Å from C(3). A final analysis of variance between observed and calculated structure factors showed no apparent errors.

(d) $Cp^*_2Mo_2(B_5H_9)$, 4. The cell parameters were only consistent with the triclinic space groups $P1$ and $P\bar{1}$; the centrosymmetric choice of $P\bar{1}$ was confirmed by the success of the refinement model. All 5746 unique data were used in the least-squares refinement. Although corrections for crystal decay were unnecessary, a face-indexed absorption correction was applied. The B−H distances to H(2), H(3), and H(4) were constrained to equal within 0.01 Å; similar constraints were applied for the chemically related B−H distances to H(13) and H(53) and to the chemically related B−H distances to H(11), H(12), H(51), and H(52). The quantity minimized by the least-squares program was $\sum w(F_o^2 - F_c^2)^2$, where $w = \{[\sigma(F_o^2)]^2 + (0.0357P)^2\}^{-1}$ and $P = (F_o^2 + 2F_c^2)/3$. No correction for isotropic extinction was necessary. Successful convergence was indicated by the maximum shift/error of 0.000 for the last cycle. The largest peak in the final Fourier difference map (1.00 eÅ^{-3}) was located 0.88 Å from Mo(2). A final analysis of variance between observed and calculated structure factors showed no apparent errors.

Acknowledgment. We thank the National Science Foundation for support of this research under grant numbers DMR03-54060 and DMR04-20768, and Scott R. Wilson and Teresa Prussak-Wieckowska for collecting the X-ray crystallographic data.

Supporting Information Available: X-ray crystallographic files in CIF format for **1**−**4**. This material is available free of charge via the Internet at http://pubs.acs.org.

JA063285+

(60) Burrell, A. K.; Cotton, F. A.; Daniels, L. M.; Petricek, V. *Inorg. Chem.* **1995**, *34*, 4253−4255.